Image Watermarking by use of Digital Holography Embedded in DCT Domain

Hsuan T. Chang and Chung L. Tsan

Photonics and Information Laboratory
Department of Electrical Engineering
National Yunlin University of Science and Technology
Douliu Yunlin, 64045 Taiwan ROC

Abstract

Digital holography techniques can be utilized to implement image watermarking schemes. In a previous method proposed by Takai and Mifume [8], a watermark image is transformed into a digital Fourier hologram, which then is directly superposed on a content image to perform the embedding process. In the detection stage, the watermark is extracted based on the inverse Fourier transform and optical holography techniques. In this study, a method, in which the hologram is superposed on the discrete-cosine-transform domain of the content image, is proposed to significantly improve Takai's method. The proposed method can significantly reduce the degradation on the superposed image, which is the major drawback in Takai's method. Simulation results also demonstrate that the watermark can be successfully extracted under different kinds of attack.

Keywords: watermark, digital holography, data hiding, DCT coefficients.

March 3, 2005

1 Introduction

Due to the fast development of the communication technologies, it is very frequent to deliver data through the Internet. If the data are not protected, they will be eavesdropped without the permission of the owner. Therefore, the techniques of protecting digital rights such as the watermarking methods have been greatly developed [1], [2]. In addition to digital techniques, some optical techniques are also proposed to achieve the encryption and protection of data [3]-[7].

Recently the watermarking techniques are greatly employed in the applications of image replication and distribution. The basic idea of the image watermarking techniques is to embed some data into the plain image in visible or invisible way to claim the ownership or the rights. There are already many mature schemes developed and have been implied to real applications. Watermarking techniques can be briefly categorized into two types: the embedding in the spatial and frequency domain, in which both are performed based on the digital methodologies.

A watermark technique incorporating the optical holography was proposed by Takai and Mifume [8]. The optical holography [9] is an interference technique to record the phase and amplitude of three-dimensional objects or two-dimensional (2-D) signals. Both the amplitude and phase information are recorded as the intensity form and can be represented as a 2-D image, which is called a hologram. If the intensity signals are recorded by a charge-coupled detector (CCD) device, they can be sampled and quantized as digital forms, which is referred as to a digital hologram and can be stored in a computer. Since a random phase modulation is used in generating the digital hologram [8], the Fourier hologram becomes a noise-like pattern. Nevertheless, the image of the object can be reconstructed from the

diffusing type of the hologram on a perfect form by the CCD camera [10], [11].

Takai's method transforms the watermark into the digital hologram pattern, which then is hidden into the content image. Then an optical technique is used to extract the hidden data. However, the content image has to be low-pass filtered to remove the low-frequency components of the content image before the watermark superposition stage. Therefore, the quality of the superposed image must be degraded very seriously. To overcome this problem, we here propose a method in which the low-pass filter can be discarded and thus the high quality of the superposed images can be preserved. Moreover, the different types of attack on the watermark are also performed to verify the robustness of the proposed watermarking method.

The rest of this paper is organized as follows: Section 2 briefly reviews the digital holographic recording and reconstruction of a 2-D watermark image. Then a previous image watermarking technique based on the digital holography is described in Section 3. Section 4 deals with the proposed method that can greatly improve Takai's method. The simulation results are provided in Section 5. Finally, the conclusion is drawn in Section 6.

2 Digital Holography for Watermark Image

A. Digital Hologram Construction

Let the watermark be denoted by $g_{\text{mark}}(x, y)$, and the random phase modulated image be expressed as

$$g_o(x, y) = g_{\text{mark}}(x, y) \exp[i2\pi\phi(x, y)], \tag{1}$$

where the 2-D signal $\phi(x, y)$ is a Gaussian random number with zero mean and a unit

standard deviation. The Fourier transform of Eq. (1) is expressed by

$$G_{\text{mark}}(\xi,\eta) = \int_{-\infty}^{\infty}\int_{-\infty}^{\infty} g_o(x,y)\exp[-2\pi i(\xi x+\eta y)]\mathrm{d}x\mathrm{d}y, \tag{2}$$

Figure 1(a) shows the systematic diagram for making a digital hologram for a given watermark image. The complex image $g_o(x,y)$ shown in Eq. (1) is Fourier transformed and then interferes with a reference wave R, which is denoted as

$$R(\xi,\eta) = R_o\exp[i2\pi(a\xi+b\eta)], \tag{3}$$

where the parameters a and b are used to determine the location of the watermark image in the reconstruction plane. The detected intensity signal of the interference result is called the ordinary hologram and can be expressed by

$$\begin{aligned} H_1(\xi,\eta) &= |G_{\text{mark}}(\xi,\eta)+R(\xi,\eta)|^2 \\ &= |G_{\text{mark}}(\xi,\eta)|^2+|R(\xi,\eta)|^2 \\ &\quad +G^*_{\text{mark}}(\xi,\eta)R(\xi,\eta)+G_{\text{mark}}(\xi,\eta)R^*(\xi,\eta), \end{aligned} \tag{4}$$

where the symbol * denotes the complex conjugate. The first and second terms on the right-hand side in Eq. (4) are discarded because only the phase information recorded in the third and the fourth terms will be useful in reconstructing the watermark. That is,

$$H(\xi,\eta) = G^*_{\text{mark}}(\xi,\eta)R(\xi,\eta)+G_{\text{mark}}(\xi,\eta)R^*(\xi,\eta), \tag{5}$$

where $H(\xi,\eta)$ denotes the digital hologram, which will be hidden in the content image.

C. Watermark Reconstruction

Figure 1(b) shows how the watermark can be reconstructed from the digital hologram. Let the reference wave used in watermark reconstruction wave be denoted as $S(\xi,\eta) =$

$|S(\xi,\eta)|\exp[i2\pi\phi_s(\xi,\eta)]$. If the conditions $|S(\xi,\eta)|=1$ and $\phi_s(\xi,\eta)=0$ are satisfied, The reconstructed wave disturbance can be given by the inverse Fourier transform of Eq. (5), i.e.,

$$g_r(x,y)=\int_{-\infty}^{\infty}\int_{-\infty}^{\infty}H(\xi,\eta)\exp[2\pi i(\xi x+\eta y)]\mathrm{d}\xi\mathrm{d}\eta. \tag{6}$$

By substituting Eq. (5) into Eq. (6), we can obtain

$$g_r(x,y)=g_o^*(x-a,y-b)+g_o[-(x+a),-(y+b)]. \tag{7}$$

This expression indicates that two symmetrical watermark images appear in the reconstructed plane. The locations of two symmetrical images are at the coordinates (a,b) and $(-a,-b)$, respectively. The parameters a and b are previously assigned in the reference wave $R(\xi,\eta)$. Since the watermark image is real, the intensity signal obtained in the reconstruction plane is expressed as

$$\begin{aligned}|g_r(x,y)|^2 &= |g_o^*(x-a,y-b)|^2+|g_o[-(x+a,y+b)]|^2\\ &= |g_{\mathrm{mark}}(x-a,y-b)|^2+|g_{\mathrm{mark}}[-(x+a),-(y+b)]|^2,\end{aligned} \tag{8}$$

Note that the random Gaussian phase term $\exp[i2\pi\phi(x,y)]$ can be totally neglected. That is, the hidden image is independent of random phase modulation when the digital hologram is constructed.

3 Watermarking Based on Digital Hologram Embedding

In embedding the digital hologram into the frequency domain of an image, both the pixel values in the digital hologram $H(\xi,\eta)$ and content image $Q(\xi,\eta)$ have to be normalized

into the range [0, 1]. That is,

$$\frac{H(\xi,\eta) - H_{\min}}{H_{\max} - H_{\min}} \rightarrow H(\xi,\eta), \tag{9}$$

and

$$\frac{Q(\xi,\eta) - Q_{\min}}{Q_{\max} - Q_{\min}} \rightarrow Q(\xi,\eta), \tag{10}$$

where $H(\xi,\eta)$ and $Q(\xi,\eta)$ denote the digital hologram and content image, respectively, after normalization. Let $H_{\max}$ and $Q_{\max}$ denote the maxima of $H(\xi,\eta)$ and $Q(\xi,\eta)$, respectively, and $H_{\min}$ and $Q_{\min}$ are the minima. After the normalization process, the following conditions hold:

$$0 \leq H(\xi,\eta) \leq 1, \quad 0 \leq Q(\xi,\eta) \leq 1. \tag{11}$$

The digital hologram $H(\xi,\eta)$ is superposed onto the content image $Q(\xi,\eta)$ with a weighting factor α. The superposed image, $I(\xi,\eta)$, now becomes

$$I(\xi,\eta) = Q(\xi,\eta) + \alpha H(\xi,\eta), \tag{12}$$

By applying the inverse Fourier transform on Eq. (12), the reconstructed image is obtained as

$$g_w(x,y) = q(x,y) + \alpha g_r(x,y), \tag{13}$$

where $q(x,y)$ is the Fourier spectrum of the content image $Q(\xi,\eta)$. Equation (13) implies that the watermark information $g_r(x,y)$ will be reconstructed together with the Fourier spectrum of the content image. To prevent the overlap effect between the watermark image and the spectrum of the content image, the location of two reconstructed images should be separated using the parameters a and b defined in Eq. (3). Figure 4 shows the desirable locations for the watermarks in the reconstruction plane. If the spectrum $q(x,y)$

is restricted in the central region and $g_r(x, y)$ appears in the regions A and B, we could separate two signals in the reconstructed plane. Therefore, in order to satisfy the non-overlapping condition, a low-pass filter must be applied to the content image $Q(\xi, \eta)$ before the inverse Fourier transform. That is,

$$I(\xi, \eta) = Q_{\mathrm{LP}}(\xi, \eta) + \alpha H(\xi, \eta). \tag{14}$$

After using the inverse Fourier transform, the signal

$$g_w(x, y) = q_{\mathrm{LP}}(x, y) + \alpha g_r(x, y). \tag{15}$$

at the reconstruction plane can be obtained. Therefore, the watermark embedded in the high-frequency hologram can be successfully extracted without the interference from the low-pass filtered content image.

The quality of reconstructed images is estimated by a error parameter, σ_I [8], which is defined as

$$\sigma_I = \frac{< (I - I_{\alpha\to\infty})^2 >^{\frac{1}{2}}}{I_{\alpha\to\infty}}, \tag{16}$$

where I denotes the case of the reconstructed image in different α, and $I_{\alpha\to\infty}$ is easily obtained by removing the content image. The brackets indicate the averaging operation on all the pixel values in an image. When σ_I value is small, better quality of reconstructed image can be obtained.

The major drawback of this method is that the content image must be pre-processed by a low-pass filter before the superposition stage. Consequently, the high-frequency components of the images have been removed and the image quality could be seriously degraded, which is a limitation in real applications. It is desirable to preserve the quality of the watermarked image, especially for the cases of large weighting factors. To achieve this goal, the

watermark hologram should not be directly embedded into the image domain. Therefore, we here propose a method in which the watermark can be embedded into the transform domain of the content image.

4 Proposed Method

The basic idea of the proposed method is to superpose the hologram into the DCT domain of the content image. The two-dimensional (2-D) DCT and of an image $q(u, v)$ of size $N_1 \times N_2$ and the corresponding inverse DCT are defined as [12]

$$Q(\xi, \eta) = 4 \sum_{u=1}^{N_1-1} \sum_{v=0}^{N_2-1} q(u, v) \cos[\frac{(2u+1)\xi\pi}{2N_1}] \cos[\frac{(2v+1)\eta\pi}{2N_2}], \tag{17}$$

and

$$q(u, v) = \frac{1}{N_1 N_2} \sum_{\xi=0}^{N_1-1} \sum_{\eta=0}^{N_2-1} a(\xi) a(\eta) Q(\xi, \eta) \cos[\frac{(2u+1)\xi\pi}{2N_1}] \cos[\frac{(2v+1)\eta\pi}{2N_2}], \tag{18}$$

respectively, where

$$\begin{aligned} a(\xi) &= \begin{cases} \frac{1}{2}, & \text{for } \xi = 0 \\ 1, & \text{for } \xi = 1, 2, \ldots, N_1 - 1 \end{cases} \\ a(\eta) &= \begin{cases} \frac{1}{2}, & \text{for } \eta = 0 \\ 1, & \text{for } \eta = 1, 2, \ldots, N_2 - 1. \end{cases} \end{aligned}$$

The energy-compact property of DCT makes the low-frequency coefficients be located around the top-left corner. The magnitudes of the median- and high-frequency coefficients are relatively much smaller than that in the low-frequency ones. By modifying only the median-frequency coefficients, the reconstructed content image will be slightly degraded, while the high-frequency parts are well preserved. On the other hand, the Fourier transform of the median-frequency DCT coefficients of the original content image can depart from the reconstructed watermark images. (The magnitudes of the FT of median-frequency DCT

coefficients are very small.) The detailed procedures of the watermark embedding and extraction are given in the following subsections.

A. Watermark Embedding

Figure 5(a) shows the schematic diagram of the watermark embedding process in the proposed method. First of all, the content image is transformed into the DCT domain and represented as to the DCT coefficients. The large coefficients located around the top-left corner represent the low-frequency components of the content image, while the small coefficients located around the bottom-right corner represent the high-frequency components. To avoid seriously degrading the quality of content image, the size of hologram is half of that of the image such that only half of DCT coefficients are modified during the embedding process. Figure 6 shows the location of median frequency coefficients of the content image. Then the digital hologram is superposed on the median-frequency coefficients $Q_{\mathrm{MED}}(u,v)$ in the DCT domain. That is,

$$Q^{'}_{\mathrm{MED}}(\xi,\eta) = Q_{\mathrm{MED}}(\xi,\eta) + \alpha H(\xi,\eta). \tag{19}$$

Then the total signal $Q^{'}(\xi,\eta)$ at the DCT domain now becomes

$$Q^{'}(\xi,\eta) = Q_{\mathrm{LOW}}(\xi,\eta) + Q^{'}_{\mathrm{MED}}(\xi,\eta) + Q_{\mathrm{HIGH}}(\xi,\eta), \tag{20}$$

where $Q_{\mathrm{LOW}}(\xi,\eta)$ and $Q_{\mathrm{HIGH}}(\xi,\eta)$ denote the low- and high-frequency coefficients, respectively. Note that the normalization process denoted in Eqs. (9) and (10) are also applied to the digital hologram and DCT coefficients, respectively. By applying the inverse DCT to the total signal $Q'(\xi,\eta)$,

$$\begin{aligned} I^{'}(u,v) &= \frac{1}{N_1 N_2} \sum_{\xi=0}^{N_1-1} \sum_{\eta=0}^{N_2-1} a(\xi)a(\eta)Q^{'}(\xi,\eta) \cos[\frac{(2\xi+1)u\pi}{2N_1}] \cos[\frac{(2\eta+1)v\pi}{2N_2}] \\ &= q(u,v) + \mathrm{IDCT}\{\alpha H(\xi,\eta)\}, \end{aligned} \tag{21}$$

the superposed image $I^{'}(u,v)$, which is the counterpart to that shown in Eq. (12), can be obtained.

B. Watermark Reconstruction

Figure 5(b) shows the schematic diagram of the process for watermark reconstruction. The superposed image $I^{'}(u,v)$ is passed through the DCT first. That is,

$$Q^{'}(\xi,\eta) = 4\sum_{\xi=1}^{N_1-1}\sum_{\eta=0}^{N_2-1} I^{'}(u,v)\cos[\frac{(2\xi+1)u\pi}{2N_1}]\cos[\frac{(2\eta+1)v\pi}{2N_2}]. \tag{22}$$

The median-frequency coefficients, $Q^{'}_{\mathrm{MED}}(\xi,\eta)$, in which the digital hologram of size 128×256 was embedded, are then extracted from the same position during the embedding stage. To reconstruct the watermark image, the extracted signal $Q^{'}_{\mathrm{MED}}(\xi,\eta)$ is inversely Fourier transformed. Fourier transform to reconstruct the watermark image. The signal $g_w(x,y)$ obtained at the reconstruction plane is

$$\begin{aligned} g_w(x,y) &= \mathrm{IFT}\{Q^{'}_{\mathrm{MED}}(\xi,\eta)\} \\ &= \mathrm{IFT}\{Q_{\mathrm{MED}}(\xi,\eta)\} + \alpha g_r(x,y). \end{aligned} \tag{23}$$

Note that the positions of the reconstructed watermarks are similar to that shown in Fig. 4. The only difference is that the reconstruction plane is half size of that in Takai's method. Moreover, the low-frequency components at the reconstruction plane are greatly reduced because that the median-frequency coefficients $Q_{\mathrm{MED}}(\xi,\eta)$ are relatively much smaller than the hologram signals $\alpha H(\xi,\eta)$.

C. Comparisons

The comparisons of the proposed method with Takai's method are summarized as follows:

1. Since the hologram is embedded into the median-frequency coefficients and thus the

DC value (the average value of the image pixels) is unaltered even when the weighting factor of the hologram is one. On the other hand, in Takai's method the averaging pixel value changes when the hologram is directly embedded in to the image. This effect is especially obvious when the weighting factor is close to one. Therefore, the fidelity of the watermarked image of the proposed method is expected to be better than that of the previous one.

2. The low-pass filter used in Takai's method degrades the content image a lot. It is eliminated in the proposed method because the superposed hologram only affects the median-frequency coefficients of the content image. In watermark reconstruction stage, there few low-frequency components appear in the reconstruction plane. It makes the watermark detection more easier than that in Takai's method.

3. Digital implementation of the DCT operation in the proposed method is easier than that of the discrete Fourier transform, which is also required for the ideal low-pass filtering in the frequency domain in Takai's method.

5 Simulation Results

Figures 7(a) and 7(b) show the two 2-D patterns selected as the watermark (a university logo) and content images, respectively. The sizes of content image and the watermark are 256×256 and 128×256 pixels, respectively. Both are 8-bit gray-level images. The PSNR value of the watermarked image and the error parameter σ_I denoting the quality of extracted watermark are used to evaluate the performance of both methods.

Figure 3(a) shows the digital hologram that is transformed from the watermark image shown in Fig. 7(a). Because the original pattern is modulated by the random Gaussian

phase, it becomes a diffuse-type image. The whole region of the image is uniform distribution. Nevertheless, a fine reconstructed image is obtained as shown in Fig. 3(b). The university logo is a symmetrical pattern obviously and does not interfere with the random phase.

A. PSNR Comparison of Watermarked Content Images

In the watermark embedding stage, Takai's method directly superpose the hologram into the image domain, while the proposed method superposes the hologram into the median-frequency coefficients of the DCT domain of the content image. The PSNR performances of the watermarked content image obtained from the previous and proposed methods are investigated. Tables 1 and 2 show the PSNR comparison of the watermarked content images (Sailor and Baboon) under different α values in the proposed and Takai's methods. For Takai's method, the PSNR are low under large α values. When $\alpha = 1$, the PSNR is 23 dB only. That is, the superposed image is significantly degraded by the insertion of digital hologram. On the other hand, all the PSNR values of the proposed method are above 40 dB even when the α values is one. Obviously, the proposed method can successfully preserve the visual quality of the watermarked content image even when a large weighting factor α is employed to increase the watermark robustness.

Figure 8 shows the watermarked content images and the watermark images located in the reconstruction plane. In the central part of the reconstruction plane, the bright low-frequency part is caused by the content image, which has been low-pass filtered before the watermark embedding stage. Because of the low-pass filtering, the watermark image can be correctly retrieved without the interference. However, it loses the high frequency components of the original content image. Therefore, the quality of content image is significantly

degraded. Moreover, for the large values of the weighting factors, such as 1, 1/2 and 1/5, the content image are blurred by the digital hologram. Thus the values of the weighting factor for the digital hologram must be as small as 1/10, 1/20, and 1/50.

The proposed method can solve the above problem. No matter the values of α are large or small, the superposed digital hologram does not blur the content image. The major reason is that the most of the energy of the content image is located in the low frequency region of the DCT domain. Since the watermark information is hidden in median-frequency region, the digital hologram does not affect the low-frequency region of the superposed image. Before performing the inverse DCT, the normalized coefficients at the low and high frequency regions are inversely normalized to become original version. The median-frequency coefficients where the digital hologram added are not changed. This procedure can avoid blurring the superposed image and thus we can obtain high PSNR values for the watermarked content image.

B. Watermark Extraction

Figures 8 and 9 show the digital watermark images reconstructed by the Takai's and proposed methods under the different α values. As shown in both figures, Takai's method has a bright area in the center (low frequency) region, but for the proposed method only a white point appears at the center of reconstructed image. The reason is that in the proposed method the watermark image is inserted into the median frequency coefficients, which are usually much smaller than the low-frequency coefficients. Therefore, the image reconstructed from the extracted median-frequency coefficients almost contains only the high-frequency hologram components, i.e., the watermark image information. For this reason, after passing $I'(u, v)$ through inverse Fourier transform, the reconstructed image

does not have a large bright pattern in the center region. Tables 1 and 2 also show that the error parameters σ_I of the extracted watermarks in the proposed method are all smaller than that in Takai's method. The proposed method not only increases the discrimination of the watermark and the low-frequency component of the content image in the reconstructed image, but also enhances the extracted watermark quality.

The application of watermark technique we presented here is not only applied to binary patterns but also halftone images. The halftone Lena image shown in Fig. 10(a) of size 64×64 is used as the watermark in the proposed method. All of the watermark embedding and extraction procedures are the same as that shown above. Let the α value be 1/5 during the computer experiment. Figure 10(b) shows the halftone wateramrk images can be successfully extracted. The Baboon image which contains much more high frequency components is used to test the proposed method. Figures 11(a)–(e) show that the embedded watermarks can be successfully extracted no matter how large the weighting factors are used.

D. Watermark Attack

The robustness of the proposed watermarking method is also investigated. First of all, Gaussian noise is added into the watermarked image. Consider the cases of two different weighting factors $\alpha = 1$ and $\alpha = 1/50$. Figures 12(a) and 12(b) show the extracted watermark images, which are clear enough. The case of tampering modification on the watermarked image is also considered here. Figure 13(a) shows another content image, in which the watermark is embedded. Figures 13(b) and 13(c) show that the clock in the image has been artificially removed and the reconstructed watermark image is still recognizable. Consider that only half of the content image is left. Figures 14(a) and 14(b) show the

half image and the reconstructed result, respectively. If the content image is blurred by Gaussian low pass filter. Figures 15(a) and 15(b) show the low-pass filtered content image and extracted watermark image, respectively. Consider the cases when the graylevels in the content image shown in Fig. 16(a) are uniformly increased and decreased. Figures 16(b) and 16(d) shows that the pixels values of the content image have been uniformly increased and decreased by 45, respectively. The corresponding watermarks are extracted and shown in Figs. 16(c) and 16(e), respectively.

6 Conclusion

A watermarking method based on the optical holography and digital image processing techniques is proposed in this paper. The watermark image is recorded into a digital hologram and then superposed into the DCT coefficients of the content image. According to the simulation results, the proposed method achieves great improvement from the previous digital-hologram-based watermarking method. The PSNR values of the watermarked content images are high even when large weighting factors α for the watermark are employed. On the other hand, the watermark image can be successfully recovered from suffering different kinds of attacks on the watermarked content image. A study for the robustness to data compression, which is the major limitation of this study, will be investigated in our future work.

References

[1] L. Cox, J. Kilian, T. Leighton,and T. Shamoon, "Secure spread spectrum watermarking for multimedia," Technical Report, 95–10, NEC Research Institute, Princeton, N.J., 1995

[2] C. I. Podilchuk and E. J. Delp, "Digital Watermarking: Algorithms and Application," IEEE Signal Processing Magazine, **18**(4), 33–46 (2001)

[3] N. Towghi, B. Javidi and Z. Lou, "Fully phase encrypted image processor," J. Opt. Soc. Am, A **16**, 1915–1927 (1999)

[4] C.H. Yeh, H.T. Chang, H.C. Chien, and C.J. Kuo, "Design of cascaded phase keys for hierarchical security system," Appl. Opt. **41**(29), 6128–6134 (2002)

[5] H.T. Chang, W.C. Lu, and C.J. Kuo, "Multiple-phase retrieval for optical security systems using random phase encoding," Appl. Opt. **41**(23), 4825–4834 (2002)

[6] K.H. Lin, H.T. Chang, W.N. Lai, and C.H. Chuang, "A public-key-based optical image cryptosystem with data embedding techniques," Opt. Eng. **42**(8), 2331–2339 (2003)

[7] Y.C. Chang, H.T. Chang, and C.J. Kuo, "Hybrid image cryptosystem based on dyadic phase displacement in the Fourier domain," Opt. Comm. **236**(4-6), 245–257 (2004)

[8] N. Takai and Y. Mifume, "Digital watermarking by a holographic technique," Appl. Opt. **41**(5), 865–873 (2002)

[9] J.W. Goodman, *Introduction to Fourier Optics*, 2nd Ed., Chap. 8, 198–254, McGraw-Hill, San Francisco (1996)

[10] I. Yamaguchi and T. Zhang, "Phase-shifting digital holography," Opt. Lett. **22**, 1268–1270 (1997)

[11] E. Tajahuerce, O. Matoba, S. C. Verrall, and B. Javidi, "Opto-electronic information encyption with phase-shifting interferometry," Appl. Opt. **39**, 2313–2320 (2000)

[12] J.S. Lin, *Two-dimensional signal and image processing*, Prentice-Hall, Inc., Chap. 3, 154–156 (1990)

Table 1: The PSNR (in dB) and σ_I comparisons under different α values for the Sailor image.

	Takai's method		Proposed method	
α	PSNR	σ_I	PSNR	σ_I
1/1	23.06	0.38	41.34	0.37
1/2	25.89	0.45	41.78	0.44
1/5	31.83	0.51	42.07	0.51
1/10	35.44	1.56	42.76	1.43
1/20	37.20	4.11	43.58	3.87
1/50	37.90	7.64	44.88	7.19

Table 2: The PSNR (in dB) and σ_I comparisons under different α values for the Baboon image.

	Takai's method		Proposed method	
α	PSNR	σ_I	PSNR	σ_I
1/1	20.06	0.41	38.24	0.39
1/2	23.96	0.48	39.22	0.48
1/5	27.31	0.55	39.87	0.56
1/10	30.21	1.77	40.49	1.56
1/20	34.55	4.71	41.29	4.22
1/50	35.10	8.22	42.36	7.54

.

Figure Captions:

Figure 1 (a) Procedure for making a digital hologram $H(\xi, \eta)$; (b) Watermark image reconstructed form digital hologram.

Figure 2 Schematic diagram of Takai's method: (a) watermark embedding; (b) watermark extraction.

Figure 3 (a) The digital hologram in which the watermark has been hidden. (b) The watermark images reconstructed from the hologram.

Figure 4 The watermark positions in the reconstructed plane.

Figure 5 Schematic diagram of the proposed method: (a) watermark embedding; (b) watermark extraction.

Figure 6 The region of median-frequency coefficients for embedding the digital hologram.

Figure 7 (a) The watermark image to be embedded and (b) the content image.

Figure 8 Simulation results of Takai's method. Upper row shows the supposed image $I(\xi, \eta)$ and lower row shows the reconstructed images $g_r(x, y)$. (a) $\alpha = 1/1$, $\sigma_I = 0.38$; (b) $\alpha = 1/5$, $\sigma_I = 0.51$; (c) $\alpha_I = 1/10$,$\sigma_I = 1.56$; (d) $\alpha = 1/50$, $\sigma_I = 7.64$.

Figure 9 Simulation result of the proposed method. Upper row shows the superposed images $I(\xi, \eta)$ and lower row shows the reconstructed images $g_r(x, y)$. (a) $\alpha = 1/1$, $\sigma_I = 0.37$; (b) $\alpha = 1/5$, $\sigma_I = 0.51$; (c) $\alpha = 1/10$, $\sigma_I = 1.43$; (d) $\alpha = 1/50$, $\sigma_I = 7.19$.

Figure 10 (a) A halftone image is used as a watermark. (b) The experiment result of the extracted watermark. (b) $\sigma_I = 0.5$.

Figure 11 (a)The original Baboon image; (b) watermarked image with the weighting factor $\alpha = 1$; (c) reconstructed watermark images, $\sigma_I = 0.55$; (d) watermarked image with the weighting factor $\alpha = 1/50$; (e) reconstruct watermark images, $\sigma_I = 7.81$.

Figure 12 The experiment result under Gaussian noise attack, (a) $\alpha = 1/1$, $\sigma_I = 8.41$ (b) $\alpha = 1/50$, $\sigma_I = 9.87$.

Figure 13 Another image shown in (a) is used as the content image. A modified image shown in (b) is suffering from the tampering modifications. (c) The extracted watermark from the experiment result. (c) $\sigma_I = 8.98$.

Figure 14 Simulation result of the proposed method: (a) Lower half image is lost; (b) The extracted watermark with $\sigma_I = 10.58$.

Figure 15 (a) The superposed image after low-pass filter; (b) The watermark reconstructed from the superposed image, $\sigma_I = 8.95$.

Figure 16 (a) Superposed image; (b) brightened image; (c) reconstruct from brightened image, $\sigma_I = 8.87$; (d) darken image; (e) reconstruct from darken image, $\sigma_I = 8.62$.

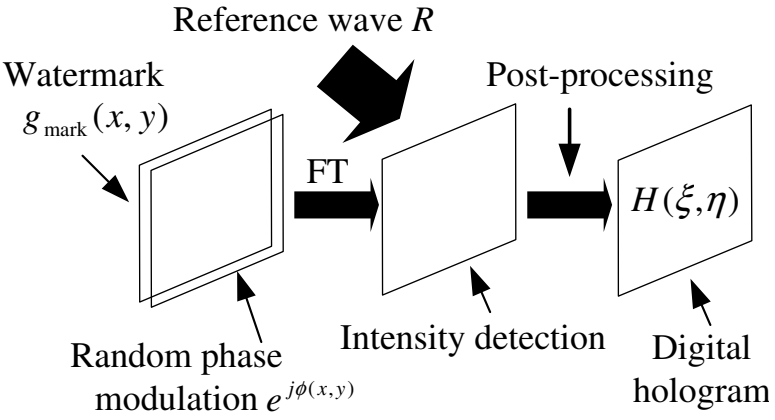

(a)

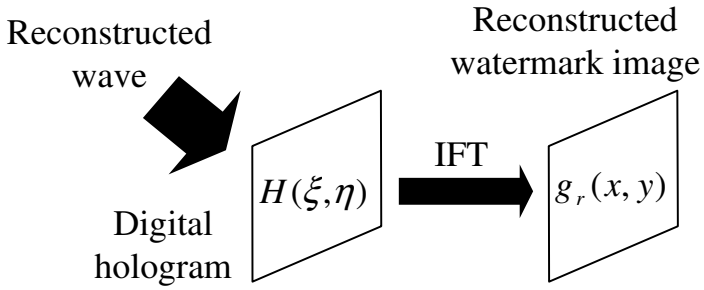

(b)

Figure 1: (a) Procedure for making a digital hologram $H(\xi, \eta)$; (b) Watermark image reconstructed form digital hologram.

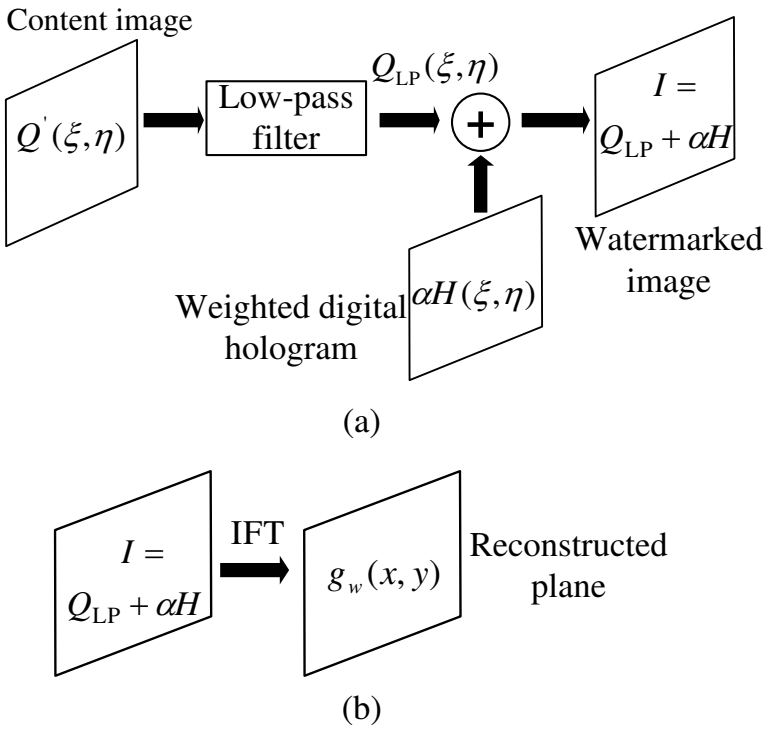

Figure 2: Schematic diagram of Takai's method: (a) watermark embedding; (b) watermark extraction.

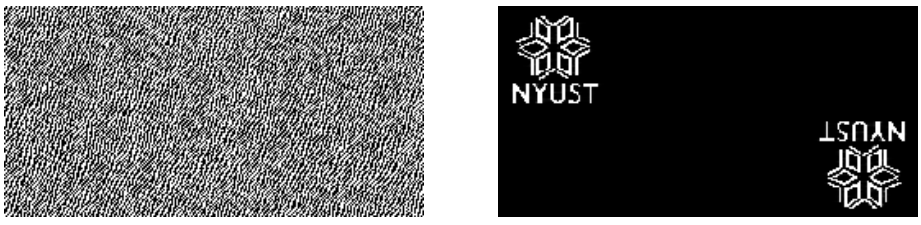

(a) (b)

Figure 3: (a) The digital hologram in which the watermark has been hidden. (b) The watermark images reconstructed from the hologram.

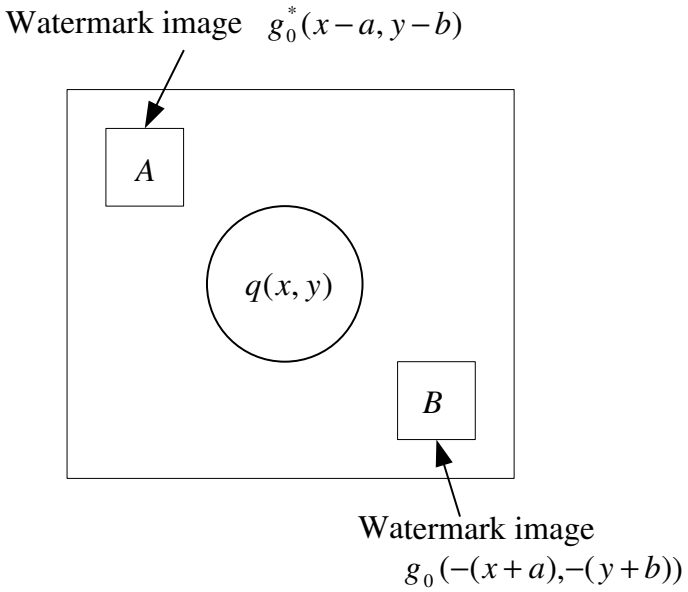

Figure 4: The watermark positions in the reconstructed plane.

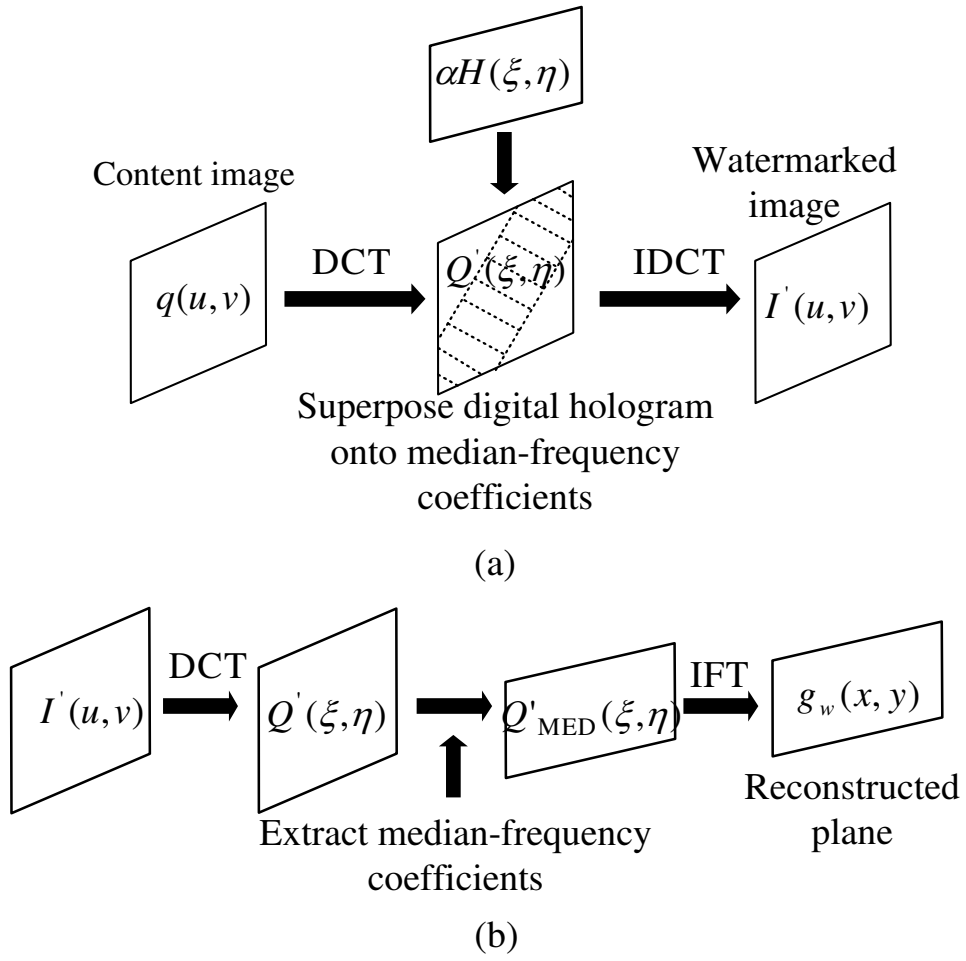

Figure 5: Schematic diagram of the proposed method: (a) watermark embedding; (b) watermark extraction.

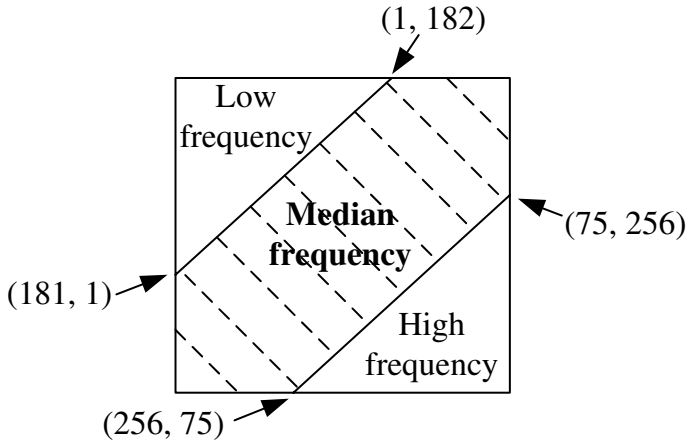

Figure 6: The region of median-frequency coefficients for embedding the digital hologram.

(a) (b)

Figure 7: (a) The watermark image to be embedded and (b) the content image.

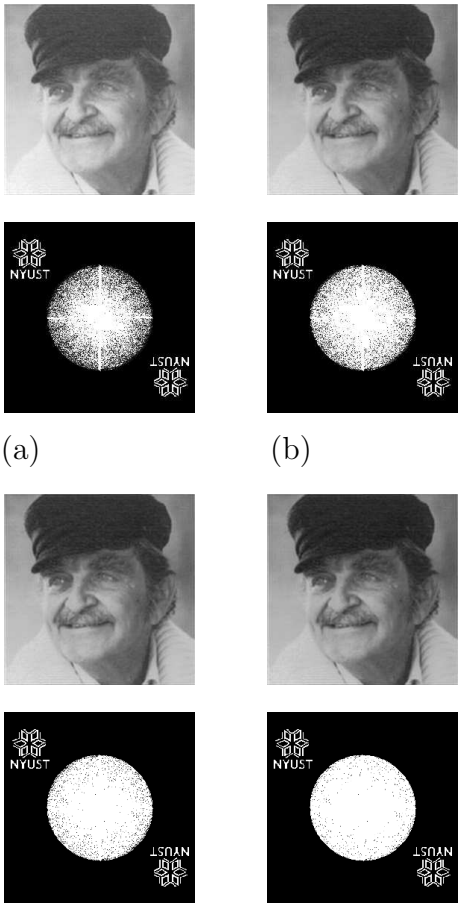

(a) (b)

(c) (d)

Figure 8: Simulation results of Takai's method. Upper row shows the supposed image $I(\xi, \eta)$ and lower row shows the reconstructed images $g_r(x, y)$. (a) $\alpha = 1/1$, $\sigma_I = 0.38$; (b) $\alpha = 1/5$, $\sigma_I = 0.51$; (c) $\alpha_I = 1/10$,$\sigma_I = 1.56$; (d) $\alpha = 1/50$, $\sigma_I = 7.64$.

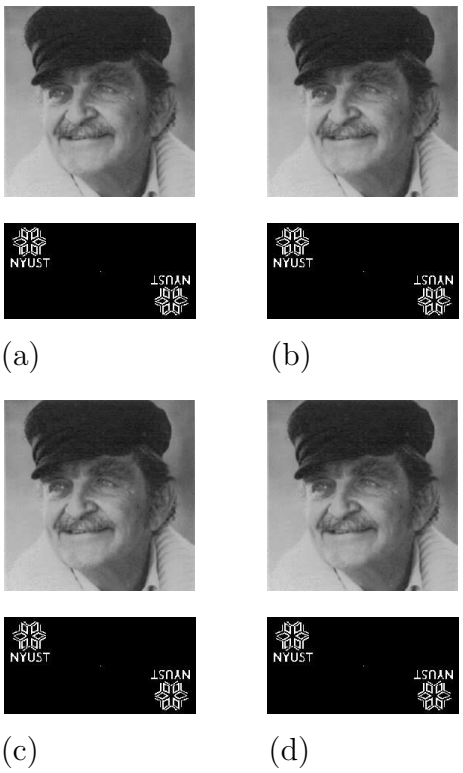

(a) (b)

(c) (d)

Figure 9: Simulation result of the proposed method. Upper row shows the superposed images $I(\xi, \eta)$ and lower row shows the reconstructed images $g_r(x, y)$. (a) $\alpha = 1/1$, $\sigma_I = 0.37$; (b) $\alpha = 1/5$, $\sigma_I = 0.51$; (c) $\alpha = 1/10$, $\sigma_I = 1.43$; (d) $\alpha = 1/50$, $\sigma_I = 7.19$.

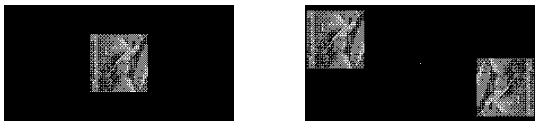

(a) (b)

Figure 10: (a) A halftone image is used as a watermark. (b) The experiment result of the extracted watermark. (b) $\sigma_I = 0.5$.

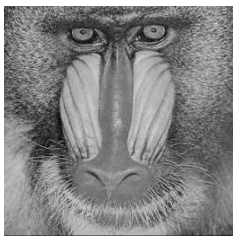

(a)

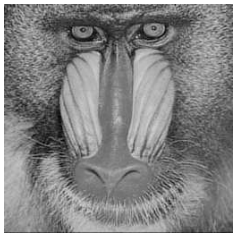

(b)

(c)

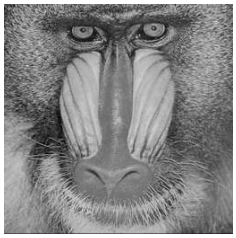

(d)

(e)

Figure 11: (a)The original Baboon image; (b) watermarked image with the weighting factor $\alpha = 1$; (c) reconstructed watermark images, $\sigma_I = 0.55$; (d) watermarked image with the weighting factor $\alpha = 1/50$; (e) reconstruct watermark images, $\sigma_I = 7.81$.

(a)

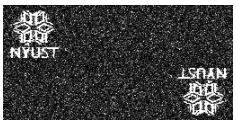

(b)

Figure 12: The experiment result under Gaussian noise attack, (a) $\alpha = 1/1$, $\sigma_I = 8.41$ (b) $\alpha = 1/50$, $\sigma_I = 9.87$.

(a) (b) (c)

Figure 13: Another image shown in (a) is used as the content image. A modified image shown in (b) is suffering from the tampering modifications. (c) The extracted watermark from the experiment result. (c) $\sigma_I = 8.98$.

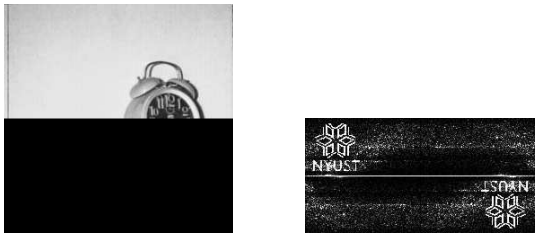

(a) (b)

Figure 14: Simulation result of the proposed method: (a) Lower half image is lost; (b) The extracted watermark with $\sigma_I = 10.58$.

(a) (b)

Figure 15: (a) The superposed image after low-pass filter; (b) The watermark reconstructed from the superposed image, $\sigma_I = 8.95$.

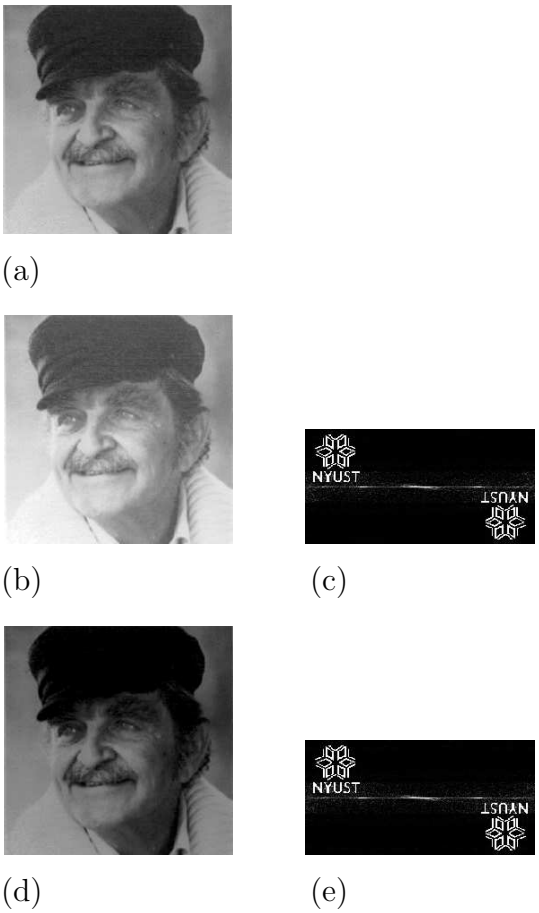

(a)

(b) (c)

(d) (e)

Figure 16: (a) Superposed image; (b) brightened image; (c) reconstruct from brightened image, $\sigma_I = 8.87$; (d) darken image; (e) reconstruct from darken image, $\sigma_I = 8.62$.